



# OPEN Identification of superficial invasive and indolent lymphomatous lymph nodes by multiple ultrasonographic vascular imaging

Lin Li<sup>1,3</sup>, Wenjuan Lu<sup>1,3</sup>, Hongyan Deng<sup>2</sup>, Wenqin Chen<sup>1</sup>, Hua Shu<sup>2</sup>, Pingyang Zhang<sup>1</sup>✉ & Xinhua Ye<sup>2</sup>✉

This study aimed to explore whether superficial invasive lymphomas and indolent lymphomas could be identified by Ultrasonographic vascular imaging. A retrospective study enrolled 82 lymphoma patients. According to proliferation rates and clinical course, the lymph nodes were classified as invasive and indolent lymphomatous lymph nodes. All patients underwent ultrasound (US) with three established techniques: color Doppler flow imaging (CDFI), angio plus ultrasound imaging (AngioPLUS™), and contrast-enhanced ultrasound (CEUS). Qualitative and quantitative parameters from the two groups were compared. Finally, the area under the receiver-operating characteristic (ROC) and regression analysis were used to compare the differences between the two groups and determine the diagnostic efficiency of the three techniques for differentiating invasive lymphoma from indolent lymphoma. The types of blood flow distribution between invasive and indolent lymphomatous lymph nodes were statistically different in all three Ultrasound techniques. In CDFI, invasive or indolent lymphomatous lymph nodes were determined by resistance index (RI) ( $p < 0.001$ ). AngioPLUSTM offered better blood flow performance and diagnostic sensitivity than CDFI. In CEUS, the differences between the two groups in necrosis and arrival time (ATM) ( $p = 0.026, 0.043$ ) were statistically significant. Finally, CDFI combined with CEUS had the highest diagnostic sensitivity of 98.1%. Interobserver agreements for qualitative parameters were all excellent. Ultrasonographic Vascular imaging is useful in identifying invasive and indolent lymphomatous lymph nodes, and CDFI combined with CEUS had the highest diagnostic sensitivity, which can guide clinicians to make more accurate diagnosis and better treatment for patients.

**Keywords** Color Doppler flow, Angio plus, CEUS, Lymphoma, Aggressiveness

According to the fifth edition of the World Health Organization Classification of Lymphoid Neoplasms of the Haematological System, lymphomas can be divided into more than 100 subtypes<sup>1</sup>. Based on the proliferation rates and clinical course, they are broadly divided into invasive and indolent lymphomas<sup>2</sup>. Clinically, transformation may occur in various low-grade indolent non-Hodgkin's lymphomas (NHL), which is defined as the progression from a histologically indolent lymphoma to a more invasive lymphoma. In this stage of the disease, there are different types of lymphomas in the body (FL with DLBCL, etc.). This transformation is associated with disease progression and poor prognosis<sup>3</sup>. Obtaining specific tissues to produce pathological findings is currently the predominant method of diagnosing lymphoma. However, simply obtaining the most accessible lymph node may not establish the diagnosis as transformation usually only occurs in part of lymph nodes or extranodal sites<sup>4</sup>. Consequently, it is necessary to determine the radiological presentation of invasive lymphoma to select biopsy sites and subsequent treatment.

PET/CT has been proven helpful in identifying transformed lymph nodes with clinical signs<sup>5</sup>. However, its high cost and ionizing radiation are a deterrent for some patients. Besides, current studies have shown that PET/CT accuracy for indolent lymphoma is suboptimal (sensitivity: 68%, specificity: 72%)<sup>6</sup>. So, the attention is focused on a non-invasive and easy-to-use diagnostic technique, which is ultrasonographic vascular imaging.

<sup>1</sup>Department of Cardiovascular Ultrasound, Nanjing First Hospital, Nanjing Medical University, Nanjing, Jiangsu, China. <sup>2</sup>Department of Ultrasound, The First Affiliated Hospital of Nanjing Medical University, 300 Guangzhou Road, Nanjing 210029, China. <sup>3</sup>Lin Li and Wenjuan Lu contributed equally to this work and share first authorship. ✉email: zhpy28@126.com; ultrasoundye@163.com

Based on the pathophysiological background, angiogenesis has a vital role in lymphoma biology, and lymphoma subtypes differ significantly in terms of angiogenesis<sup>7–10</sup>. Menzel et al.<sup>11</sup> found that the progression of invasive lymphoma is usually accompanied by a so-called "vascular phase," which represents extensive vascularization of the lymph nodes, with the exponential growth of the internal vessels and no intervals, while indolent lymphomas are well differentiated, with relatively normal blood flow. Hence, we focus on the advantages of ultrasonographic Vascular imaging for qualitative and quantitative assessment of lymph node blood flow. The techniques include color Doppler flow (CDFI), angio plus ultrasound imaging (AngioPLUS™), and contrast-enhanced ultrasound (CEUS). It was proved that CDFI is helpful to the differential diagnosis of superficial enlarged lymph nodes and to reflect the aggressiveness of lymphoma<sup>12</sup>. AngioPLUS maximizes the velocity resolution of blood flow with a detailed resolution of up to 50 microns, which can detect the tiny vessels<sup>13</sup>. And CEUS combines real-time visualization of microvascular perfusion in nodules and time-intensity curve (TIC) analysis to provide an objective and quantitative way to analyze perfusion characteristics of lymph nodes<sup>14,15</sup>.

Therefore, this study evaluated whether ultrasonographic vascular imaging could help differentiate superficial lymph nodes of different WHO lymphoma subtypes, thus providing preliminary insights for clinical biopsy.

## Materials and method

All the qualitative and quantitative indicators of ultrasonographic vascular imaging were assessed by two radiologists with more than five years of experience.

### Patients

We conducted a retrospective analysis of 116 patients between September 2020 and November 2022, who underwent ultrasonographic vascular imaging for superficial enlarged lymph nodes. Then, 34 patients were further excluded based on the following exclusion criteria: selected lymph nodes without pathological confirmation ( $n=12$ ); fused lymphomas ( $n=6$ ); interval between US examination and histopathology more than 60 days ( $n=0$ ); pregnant or breast-feeding women ( $n=0$ ); prior chemotherapy/radiation therapy ( $n=5$ ); contrast allergy ( $n=3$ ); severe comorbidities ( $n=8$ ); those with more than one histologically subtype of NHL or coexistence of Hodgkin's disease and NHL ( $n=0$ ). Inclusion required adults ( $\geq 18$  years) with histopathologically confirmed lymphoma; superficial lymph nodes (neck, axillary, inguinal) showing high uptake on PET/CT. Ultimately, 82 patients with 82 lesions were enrolled in the study with an effect size of 0.5,  $\alpha=0.05$ , and power=0.8, which exceeded calculated minimum sample size 64. Diagnosis adhered to the 5th WHO Classification of Lymphoid Neoplasms (2022)<sup>1</sup>. Pathologists classified lymphomas as invasive (e.g., DLBCL, ALCL) or indolent (e.g., FL, MZL) based on proliferation rates and clinical behavior<sup>2</sup>. Recruitment followed institutional protocols, and all participants provided informed consent. The study was approved by the Ethics Committee under ethics number 2022-SR-058. All methods were performed in accordance with the relevant guidelines and regulations. Two radiologists specializing in ultrasound independently analyzed the results of three ultrasonographic vascular imaging modalities (CDFI, AngioPLUS, and CEUS) for each lymphoma case.

### CDFI

CDFI was performed on the Aixplorer ultrasound system (SuperSonic Imagine, Aix-en-Provence, France) equipped with an SL15-4 linear transducer. The sampling frame was sized to completely encapsulate the mass. The color gain was adjusted to a level where low velocity vascular flow in the target lesion can be detected with minimal background noise. The velocity scale for color Doppler examination was 10 cm/s. Multi-sectional scanning was used to show the maximum vascular flow in the target lesion. If lymphatic hilar structures were present, they need to be adequately displayed. Patients took a supine position, breathed calmly, and fully exposed the area to be examined. The patterns of CDFI were categorized as the following four types<sup>16</sup>: (1) hilar; (2) peripheral; (3) mixed: the existence of both hilar and peripheral flow signal or scattered short rod-shaped blood flow signals; and (4) absent. The resistance index (RI) of blood flow should be measured at different sites<sup>12</sup>. Besides, the sampling volumes were all adjusted to the smallest size to avoid bias caused by different volumes sizes<sup>14</sup>.

### AngioPLUS™

AngioPLUS™ was also performed on the Aixplorer ultrasound system with SL15-4 linear transducer. The color gain and sampling frame were adjusted in line with that of the color Doppler, while the scale was set at 3 cm/s. The same lymph nodes as described above were selected for AngioPLUS™. Referring to the previous literature<sup>13,17</sup>, we assessed the microvascular condition within the lymphoma in terms of AngioPLUS amount, distribution of vessels, and Four-tier vascularity score. The number of vessels in the lymphoma could be qualitatively defined as follows: (1). Absent; (2). Minimal: 1–2 vessels within the mass or at the edge of the mass; (3). Moderate: 3–4 vessels within the mass or at the edge of the mass; (4). Marked: 5 or more penetrating vessels in the mass; The distribution of blood vessels was defined as: (1). Absent; (2). Vessels in the rim; (3). Internal blood flow: punctate or perforating vessels exist in the mass; (4). Combined. For four-tier vascularity score, we referred to the scoring method designed by Min Ji Son et al.<sup>18</sup>:

1. Score 1: no vessels; central or peripheral punctate vessels;
2. Score 2: 1 or 2 peripheral vessels that do not enter the nodes;
3. Score 3: 3 or more peripheral vessels, or 1–2 penetrating vessels;
4. Score 4: 3 or more penetrating vessels or disrupted internal blood flow.

CEUS

The LogiqE9 ultrasound machine (GE Medical Systems, Milwaukee, WI, USA) with a 9L linear transducer was used to perform the CEUS examination in MSK GEN mode. The mechanical index (MI) and thermal index (TI) was set at 0.14, 0.0 respectively. Then 5 ml of 0.9% saline was added into the contrast medium (SonoVue, Bracco, Milan, Italy) and shaken forcefully to make emulsion-like microbubbles for preparation. The patient was positioned as above, and the same lymphoma section as above is selected for observation. Afterward, 2.4 ml of contrast medium was injected rapidly into the patient's elbow vein, followed by 5 ml of saline. The timer built into the machine started simultaneously and recorded the angiography process in real-time for approximately 60 s. During this procedure, the probe was kept fixed. After the angiography, the dynamic video was saved, and the patient was closely observed for any side effects.

CEUS imaging analysis

The characteristics of lymphomas in CEUS included enhancement mode, boundary, intensity, distribution, and necrosis<sup>19,20</sup>. (1) Enhancement intensity was divided into no enhancement, low enhancement (lower than surrounding normal tissue), moderate enhancement (equal to the surrounding normal tissue), high enhancement (higher than surrounding normal tissue, but lower than surrounding arteries), and intense enhancement (equal to the surrounding arteries). (2) Enhancement distribution was classified as hilar, central (enhanced from peripheral to the interior), centrifugal (enhanced from the center to peripheral), mixed (simultaneously enhanced at the margins and the center or diffuse enhancement), and peripheral. (3) Enhancement boundary was divided into clear and unclear. (4) Enhancement patterns: homogeneous and heterogeneous.

Observe the process of lymphoma angiography and intercept the period from 1 s before the start of enhancement to 40 s of enhancement for TIC analysis, using GE LogiqE9 quantification software. The entire enhanced lymph node was selected as the region of interest (ROI). It was essential to avoid surrounding tissues and blood vessels when outlining the ROI. The parameters provided by TIC analysis had to be measured three times and averaged, including arrival time (ATM); time to peak (TP);  $\Delta T = TTP - ATM$ ; area under the gamma curve (Area); curve gradient (Grad); base intensity (BI); peak intensity (PI)<sup>19</sup>.

Histologic analysis

Experienced hematopathologists reviewed all tissue specimens at our institution. The pathological diagnosis was confirmed for all patients based on the fifth edition of the World Health Organization Classification of Lymphoid Neoplasms of the Haematological System.

Statistical analysis

SPSS software (version 21.0; IBM Corporation, NY, USA) was used for data analysis. The quantitative parameters were expressed as mean  $\pm$  SD. Statistical analysis between the two groups was done using independent samples t-test for quantitative parameters and chi-square test for qualitative parameters. Regression analysis was used to diagnose image characteristics and quantitative parameters jointly. Meaningful characteristics of each technique were chosen to assess the diagnostic efficacy of the technique. The diagnostic value of different ultrasound techniques was analyzed by the area under the receiver-operating characteristic (ROC) with the Medcalc 18.2.1.0 software.  $P < 0.05$  was statistically significant. Observer consistency was assessed using intra-group correlation (ICC) and kappa for continuous and categorical variables. Consistency was considered poor when ICC/kappa was 0–0.4; 0.4–0.59, fair; 0.6–0.74, good; and 0.75–1, excellent<sup>21</sup>.

Results

ICC

ICC and kappa values showed excellent inter-observer agreement (Table 1).

Clinical features

Eighty-two patients (37 males and 45 females; average age, 60.3 years; range, 28–88 years) with 82 lymphomatous lymph nodes were enrolled in our research. Of the 82 lymphomatous lymph nodes, there were 54 cases of invasive lymphoma (45 cases of diffuse large B-cell lymphoma, DLBCL; 3 cases of anaplastic large cell lymphoma, ALCL; 6 cases of grade III follicular lymphoma) and 28 cases of indolent lymphoma (13 cases of I-II follicular

Features	ICC/Kappa	Features	ICC/Kappa
Patterns of CDFI	0.883	AT	0.883
Amount of vessels	0.857	TP	0.882
Distribution of vessels	0.873	$\Delta T$	0.814
Four-tier vascularity score	0.903	BI	0.903
Enhancement intensity	0.878	PI	0.912
Enhancement distribution	0.801	$\Delta I$	0.857
Enhancement boundary	0.812	Grad	0.842
Necrosis	0.89	AUC	0.853
Enhancement pattern	0.855	RI	0.837

**Table 1.** Consistency of the observers with regard to US features of lymphomas.

lymphoma, FL; 11 cases of nodal marginal zone lymphoma, MZL; 2 cases of lymphoplasmacytic lymphoma, LPL; and 2 cases of B-Cell Lymphoproliferative Disease, BCLD). Besides, 54 enlarged lymph nodes were in the neck, 17 in the inguinal region, and 11 in the axillary.

CDFI and AngioPLUS™

Characteristics of CDFI and AngioPLUS™ in invasive lymphoma and indolent lymphomas are compared in Table 2. Regarding CDFI and AngioPLUS™, the blood flow distribution was significantly different between invasive lymphoma and indolent lymphomas. In invasive lymphomas, it mainly presented as “mixed” blood flow (Fig. 1) and an absence of blood flow, whereas half of the indolent lymphoma manifested as “hilar” type of blood flow ( $P=0.002$ ) (Fig. 2). Besides, “marginal” blood supply was only present in invasive lymphomas. The RI of invasive lymphoma ( $0.66 \pm 0.09$ , range 0.51–0.84) was higher than that of indolent lymphomas ( $0.56 \pm 0.07$ , range 0.41–0.69) ( $P<0.001$ ) (Fig. 3). The optimal cut-off value of RI was 0.625, with the sensitivity, specificity, accuracy and the area under the curve (AUC) of 67.4%, 84.6%, 81.3% and 0.813 respectively. AngioPLUS™ offered better performance than CDFI for all features. CDFI showed no vascularity in 1 (3.6%) of the 28 indolent lymphomas and in 9 (16.7%) of the 54 invasive lymphomas, whereas 0 (0%) of the indolent lymphomas and 2 (3.7%) of the invasive lymphomas were avascular on AngioPLUS™.

CEUS

Quantitative results of CEUS are shown in Table 3. For the optimization of the threshold values for ATM (15.058 s), differences were observed between the two groups, with the AUC of 0.636, the sensitivity of 53.6%, and the specificity of 83.3%, respectively ( $P=0.043$ ). There were no statistical differences for the remaining parameters. Qualitative findings of CEUS are summarized in Table 4. The results showed that the majority of invasive (43/54, 79.7%) and indolent (28/28, 100%) lymphomas displayed hyperenhancement, and no statistical difference was found between them ( $P=0.141$ ). Concerning enhancement distribution, invasive lymphomas (19/54, 35.2% vs. 4/28, 14.3%) showed more of a centripetal enhancement distribution. Besides, “marginal” enhancement ( $P=0.028$ ) and necrosis ( $p=0.026$ ) (Fig. 4) were only seen in invasive lymphomas.

The combination of Ultrasound techniques

The two groups’ sensitivity, specificity, and accuracy of single and multiple combined imaging techniques were compared (Table 5). The results indicated that the combination of the three had the highest diagnostic efficacy (AUC=0.941), with diagnostic sensitivity, specificity of 90.7%, 85.7%, respectively (Fig. 5). In contrast, CDFI combined with CEUS had the highest diagnostic sensitivity of 0.981. And there was no statistically significant difference in diagnostic efficacy between CDFI combined with CEUS and the combination of the three primary ultrasonographic Vascular imaging techniques ( $p=0.261$ ) (Table 6).

Characteristic	Pathology type		P value
	Invasive lymphoma (n = 54)	Indolent lymphoma (n = 28)	
RI	0.66 ± 0.09	0.56 ± 0.07	< 0.001
Patterns of CDFI			
Absent	9 (16.7%)	1 (3.6%)	0.002
Hilar	10 (18.5%)	14 (50.0%)	
Mixed	25 (46.3%)	13 (46.4%)	
Peripheral	10 (18.5%)	0 (0.0%)	
Amount of vessels			
Absent	2 (3.7%)	0 (0.0%)	0.185
Minimal	10 (18.5%)	1 (3.6%)	
Moderate	12 (22.2%)	7 (25.0%)	
Marked	30 (55.6%)	20 (71.4%)	
Distribution of vessels			
Absent	2 (3.7%)	0 (0.0%)	0.024
Internal vascularity	7 (13.0%)	10 (35.7%)	
Vessels in rim	11 (20.4%)	1 (3.6%)	
Combined	34 (63.0%)	17 (60.7%)	
Four-tier vascularity score			
1	6 (11.1%)	0 (0.0%)	0.115
2	10 (18.5%)	2 (7.1%)	
3	16 (29.6%)	12 (42.9%)	
4	22 (40.7%)	14 (50.0%)	

Table 2. CDFI and AngioPLUS in 82 Invasive and Indolent lymphomas.



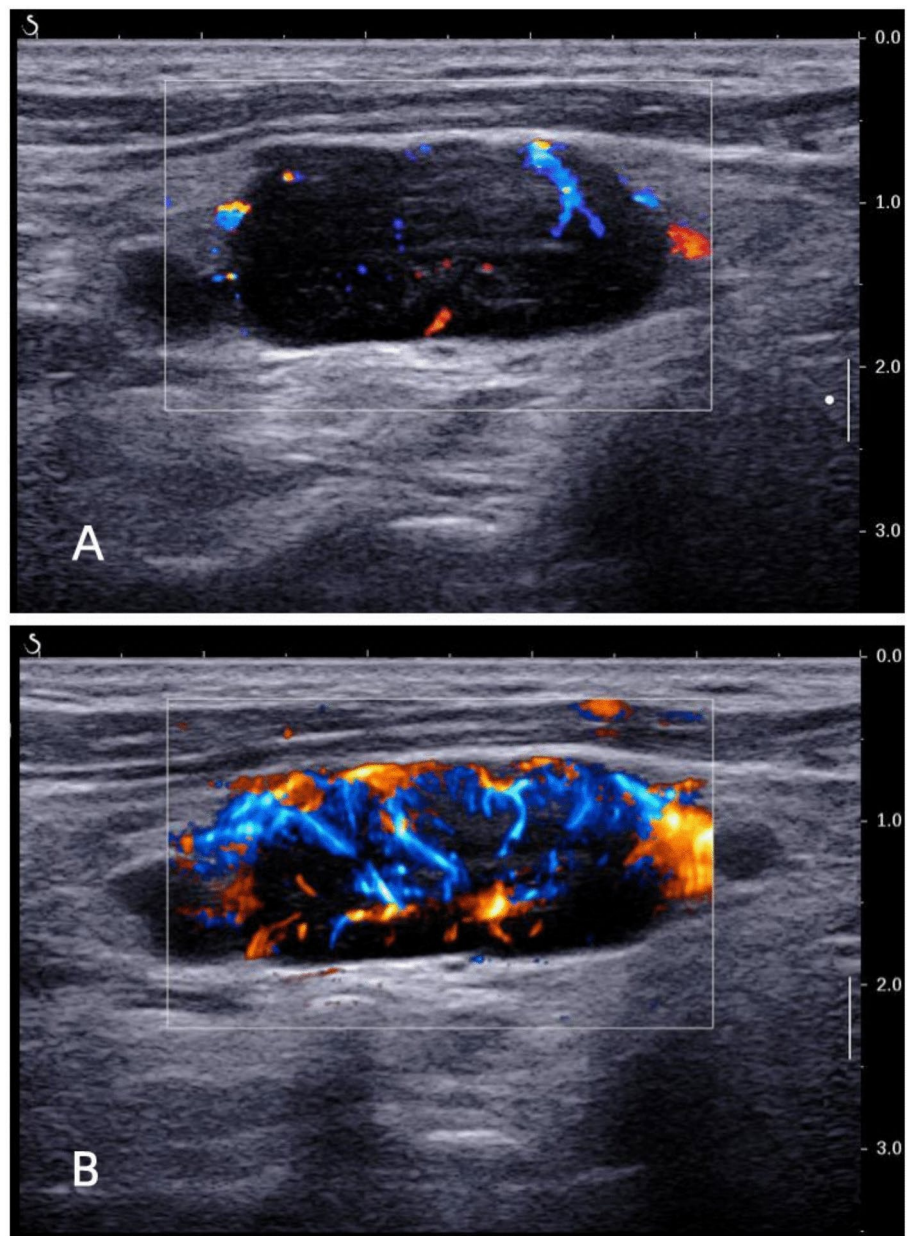


**Fig. 1.** (A) Invasive lymphoma appears on CDFI as a punctate “central” blood flow with a bit of “Peripheral” blood flow signal. (B) On AngioPLUS, the same lymphoma shows an abundant “mixed” blood flow signal.

## Discussion

There is growing evidence of a correlation between the type of vascular condition and the aggressiveness of lymphomas<sup>7,22,23</sup>. To identify signs of transformation and to identify potential biopsy sites, this retrospective study was designed to clarify invasive and indolent Lymphomatous lymph nodes through Ultrasonographic Vascular imaging, which finally impact the selection of treatment programs.

The three ultrasound techniques, including CDFI, AngioPLUS™, and CEUS, are all capable of showing vascular distribution. The results indicated that indolent lymphomas presented more often with “hilar” and “centrifugal” blood flow types, while invasive lymphomas had a greater distribution of “mixed” and “central”. This is consistent with previous research findings<sup>24,25</sup>. Besides, “peripheral” blood flow type was only found in invasive lymphomas. In line with this, Giovagnorio et al.<sup>26</sup> found that six lymphomas showing “peripheral” vessels pathologically were all confirmed as high-grade invasive lymphoma. In conclusion, there is a correlation between the type of vascular distribution and the tissue aggressiveness of the lymphoma. In terms of biological behavior, lymphoma center is initially infiltrated by tumor cells. But indolent lymphoma is slow to develop, so the surrounding area may remain untouched for a long time. As the inside-out invasion of the tumor cells, microinfiltrates may have developed in the surrounding areas, but CDFI cannot detect the microinfiltrates<sup>12</sup>. Thus, early lymphomas and indolent lymphomas were more likely to present a “hilar” distribution. In invasive

(B): On AngioPLUS™, the same lymphoma shows an abundant “mixed” blood flow signal.

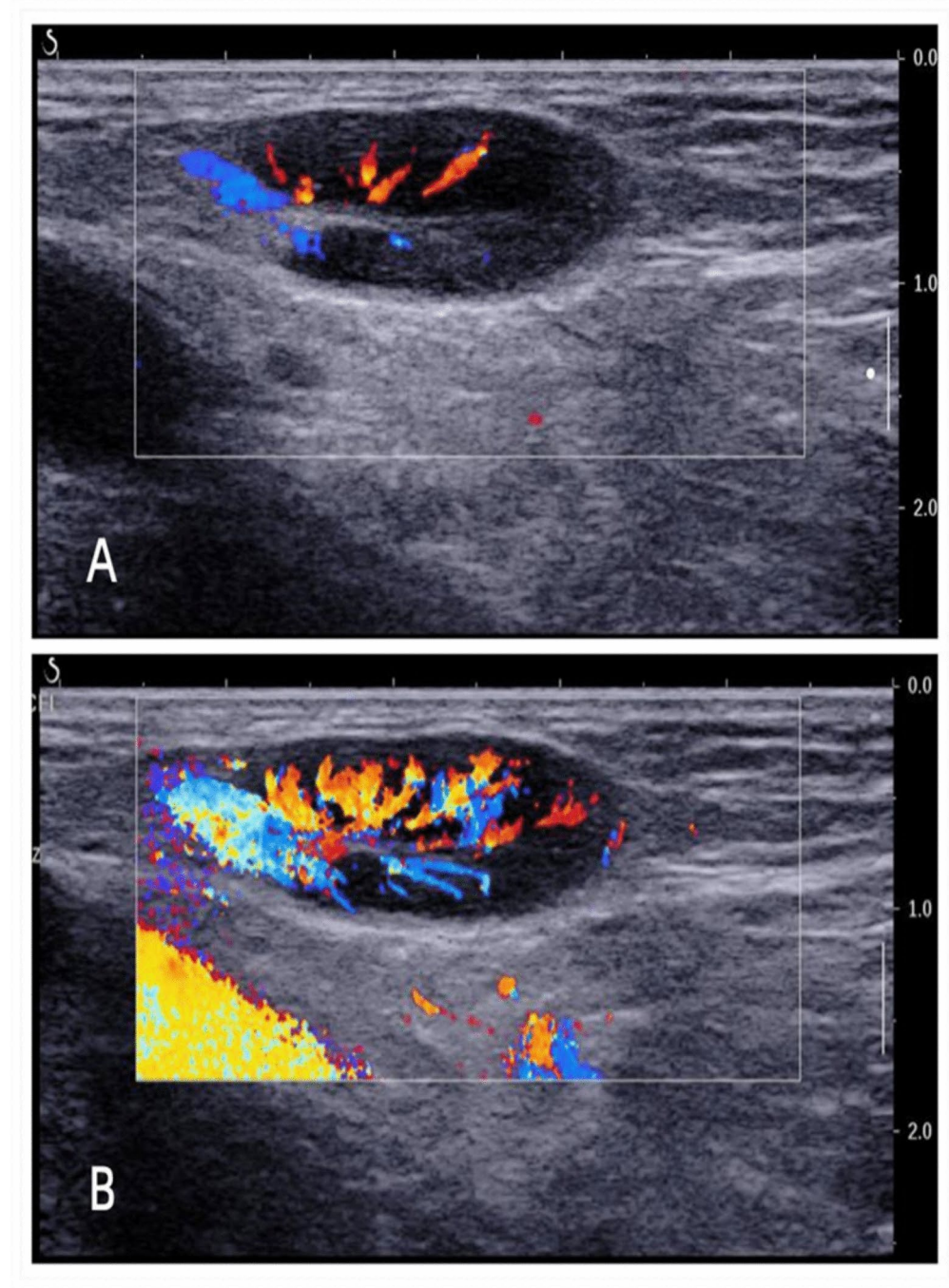


**Fig. 2.** The indolent lymphoma shows a typical “hilar” flow on CDFI (A), and the amount of flow signal is increasing on AngioPLUS (B).

lymphomas, tumor cells can even reach the lymph nodes from the external side, when the disease has its origin in another lymph node of the cluster and thereafter invades the rest of the nodes, similar to metastasis, which explains why invasive lymphomas show a predominance of “mixed” and “peripheral” distribution<sup>26</sup>.

The RI values were higher in invasive lymphoma and lower in indolent lymphoma, with optimal cut-off value of 0.625, providing sensitivity, specificity, and accuracy of 67.4%, 84.6%, and 81.3% respectively. Likewise, in the JIANG et al.<sup>19</sup> study, the RI cut-off value was 0.595, providing a sensitivity, specificity, and accuracy of 85%, 79%, and 81.5%. In molecular biology, angiogenesis and translocation of vessels occur in the course of multiplication and infiltration of malignant tumor cells. This process is accompanied either by the destruction of the basement membrane of the blood vessels or by the migration and proliferation of endothelial cells, leading to the narrowing of blood vessels and an increase in blood flow resistance<sup>27</sup>. In contrast, in early-stage lymphoma or indolent

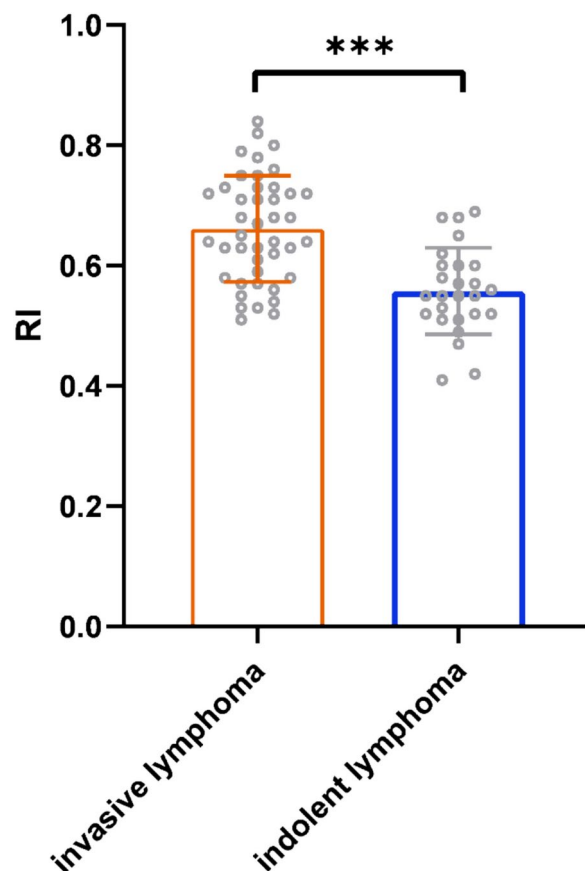


**Fig. 3.** Distribution of RI in invasive and indolent non-Hodgkin's lymphoma (NHL), demonstrating a higher RI in invasive NHL. However, in the lower RI levels, there is an overlap between invasive and indolent NHL.

Parameter	Invasive lymphoma		Indolent lymphoma		P value
	Range	Mean $\pm$ Standard Deviation	Range	Mean $\pm$ Standard Deviation	
AT	3.55–21.62	11.90 $\pm$ 3.80	5.88–21.35	13.84 $\pm$ 4.50	0.043
TP	9.22–38.77	23.3 $\pm$ 16.25	14.81–36.81	24.21 $\pm$ 6.19	0.547
$\Delta$ T	5.67–23.83	11.44 $\pm$ 3.57	6.61–16.37	10.38 $\pm$ 2.67	0.171
BI	–70.90 to –54.43	–63.18 $\pm$ 3.46	–70.50 to –57.5	–63.82 $\pm$ 3.38	0.426
PI	–60.64 to –34.31	–46.35 $\pm$ 5.52	–56.70 to –32.57	–46.46 $\pm$ 6.09	0.937
$\Delta$ I	6.96–26.84	16.82 $\pm$ 3.92	8.60–30.33	17.36 $\pm$ 4.86	0.592
Grad	0.442–3.802	1.72 $\pm$ 0.65	0.57–3.85	1.78 $\pm$ 0.75	0.891
AUC	96.41–567.958	329.36 $\pm$ 103.29	117.37–795.52	328.23 $\pm$ 143.27	0.968

**Table 3.** Qualitative results of CEUS.

lymphoma, the biological behavior of the lymphoma cells and the morphology of the vessels are similar to that of normal and, therefore, may have a lower RI. Consequently, as the aggressiveness of the lymphoma increases, the RI increases accordingly<sup>28</sup>.

In CEUS, necrosis was only observed in invasive lymphomas. Although the rate of necrosis in lymphomas is low, necrosis can occur when the growth rate of tumor cells exceeds the rate of blood supply. The presence of necrosis, in turn, is often a late event in the invasion of lymph nodes and is highly suggestive of tumor aggressiveness<sup>29</sup>. The previous paper has noted that massive necrosis suggests complete lymph node invasion by neoplastic tissue<sup>12</sup>.

Among the quantitative parameters of CEUS, ATM is shorter in invasive lymphomas (<15.058), with a low AUC of 0.636, poor sensitivity of 53.6%, and high specificity of 83.3%, respectively. This probably is related to the fact that the more advanced the stage of the tumor, or the more aggressive it is, the more vascular the tumor contains. As a result, there is an increase in blood flow velocity within the tumor and, accordingly, a shorter ATM<sup>19</sup>. However, in the previous study by Jiang et al.<sup>19</sup>, they did not find any meaningful quantitative

Characteristic	Pathology type		P value
	Invasive lymphoma	Indolent lymphoma	
Enhancement intensity			
None	0(0.0%)	0(0.0%)	0.141
Weak	3(5.5%)	0(0.0%)	
Moderate	7(13.0%)	0(0.0%)	
High	16(29.6%)	11(39.3%)	
Intense	28(51.9%)	17(60.7%)	
Enhancement pattern			
Homogeneous	23(42.6%)	18(64.3%)	0.062
Heterogeneous	31(57.4%)	10(35.7%)	
Enhancement distribution			
Hilar	11(20.4%)	11(39.3%)	0.028
Central	19(35.2%)	4(14.3%)	
Centrifugal	4(7.4%)	6(21.4%)	
Mixed	15(27.8%)	7(25.0%)	
Peripheral	5(9.3%)	0(0.0%)	
Enhancement boundary			
Clear	25(46.3%)	17(60.7%)	0.215
Unclear	29(53.7%)	11(39.3%)	
Necrosis			
Yes	11(20.4%)	0(0.0%)	0.026
No	43(79.6%)	28(100%)	

**Table 4.** Comparison of the invasive and indolent lymphoma qualitative parameters using CEUS.

parameters in the differential diagnosis of invasive and indolent lymphomas by CEUS, given that their sample size of indolent lymphomas was only 12 cases.

Although the number of vessels was not statistically different in our study, it is still an indicator we need to keep an eye on. Rich blood supply is the hallmark of malignant lymphoma<sup>30</sup>. In our study, both the indolent and invasive lymphomas had an abundant number of microvessels, and there was no statistical difference between them. Consistent with this, most lymphomas showed high enhancement in CEUS, especially indolent lymphomas, all of which exhibit hyperenhancement. Likewise, in the study by MA et al.<sup>6</sup>, four indolent lymphomas they included all showed a rapid homogenous hyper-enhanced pattern in CEUS, noting that CEUS imaging of indolent lymphomas was only affected by blood flow. Although there is massive angiogenesis within both invasive and indolent lymphomas, the vessels within the former are more immature, straggly, and tiny<sup>31</sup>. However, Over-angiogenesis is an independent marker of poorer survival in part of indolent lymphomas and may promote transformation<sup>8</sup>. Promisingly, the prediction of transformation of indolent lymphoma by angiography is a study direction.

AngioPLUS™ improves the detection of abnormal blood flow distribution in malignant lymphomas and increases the diagnostic sensitivity (87%)<sup>32</sup>, reflecting the better performance of AngioPLUS. With AngioPLUS, 18% of the lymphomas (10 cases of invasive lymphoma, 5 cases of indolent lymphoma) displayed a more complex distribution in our study. CDFI showed no vascularity in 1(3.6%) of the 28 indolent lymphomas and in 9 (16.7%) of the 54 invasive lymphomas, whereas 0 (0%) of the indolent lymphomas and 2 (3.7%) of the invasive lymphomas were avascular on AngioPLUS™. Relative to CDFI and AngioPLUS, the CEUS had the highest diagnostic specificity of 87.9%. It was also found that CEUS is less sensitive for diagnosis than AngioPLUS, which is consistent with the results obtained by Kratzer et al.<sup>33</sup> in their comparative study of AngioPLUS™ and CEUS in breast tumors. It may be that excessive contrast concentration does not match the injection rate, resulting in high contrast concentration in the target area, blurred image contrast, and reduced fine resolution<sup>34,35</sup>. Besides, the combination of the three techniques has the highest diagnostic efficacy (AUC = 0.941), with a sensitivity of 90.7%, specificity of 85.7%. CDFI combined with CEUS had the highest diagnostic sensitivity of 98.1%. Unexpectedly, there was no statistically significant difference between CDFI combined with CEUS and the combination of the three. Therefore, we recommend using CDFI in combination with CEUS to differentiate invasive and indolent lymphomas for the highest sensitivity and excellent diagnostic efficacy.

However, our study has limitations. Firstly, the sample size was relatively small, especially for indolent lymphomas. Secondly, selection bias is due to selecting only superficial lymph nodes. For the cases of deep lymph node enlargement, extra-nodal infiltration, and hepatosplenic infiltration, this is still where the limitations of ultrasonography lie. Thirdly, the parameters of TIC may be affected by many factors, including the dose of contrast, the machine, the patient's metabolism, and the speed of contrast agent injection. Fourthly, CEUS requires specifically trained operators to ensure an adequate interpretation of contrast patterns and that there are no standardized protocols to guide the performance of CEUS examinations in the lymph nodes. Therefore, ultrasonographic vascular imaging can currently only be an aid in identifying invasive and indolent lymphomatous lymph nodes. It still requires a large sample size for further study.



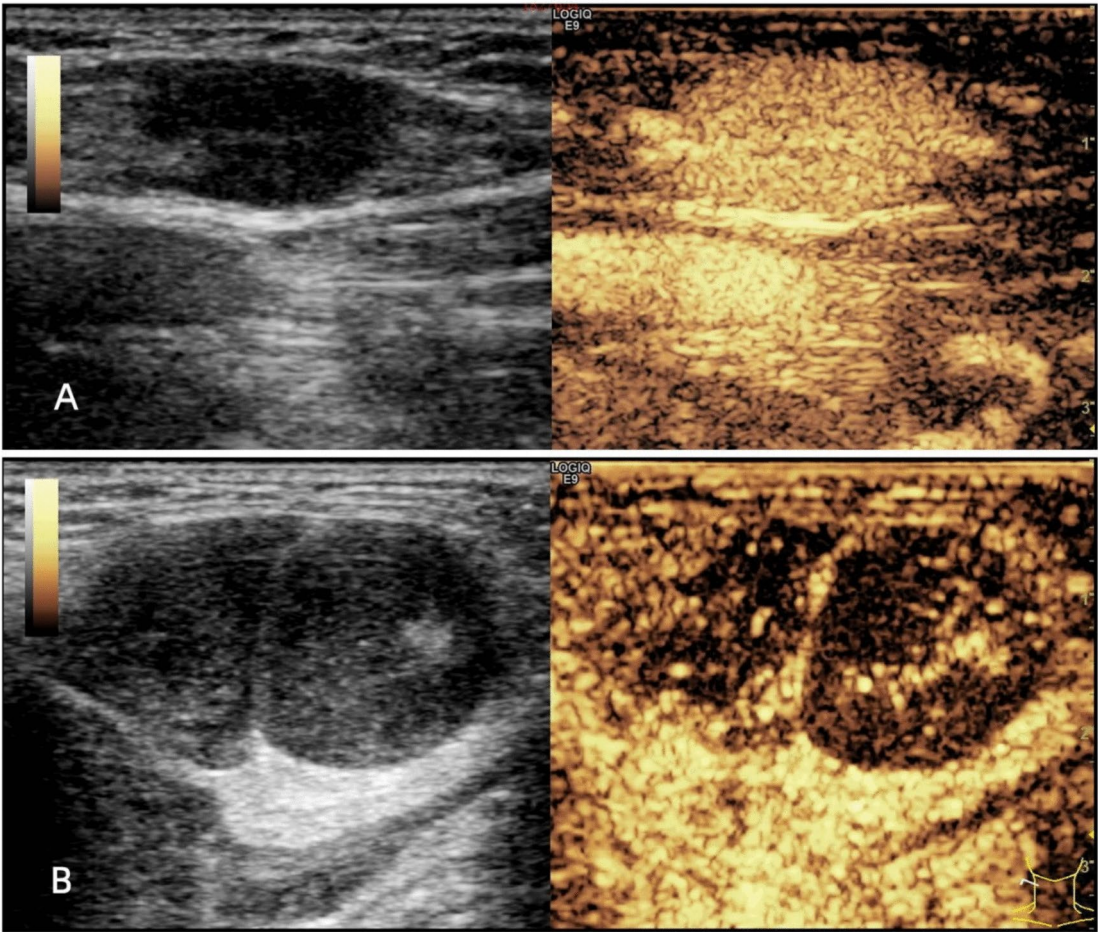


**Fig. 4.** (A): An indolent lymphoma appears as a well-defined homogeneous hyperenhancement on CEUS, suggesting that the blood supply is also abundant in indolent lymphomas. (B): Two invasive lymphomas show heterogeneous enhancement on CEUS, with a large area of necrosis.

Index	AUC	P-value	CI 95%	Sensitivity (%)	Specificity (%)
CDFI	0.808	< 0.001	0.714–0.902	0.667	0.857
AngioPLUS	0.676	0.009	0.556–0.796	0.870	0.357
CEUS	0.879	< 0.001	0.794–0.963	0.778	0.857
CDFI + CEUS	0.925	< 0.001	0.861–0.988	0.981	0.750
CDFI + AngioPLUS	0.808	< 0.001	0.714–0.902	0.667	0.857
AngioPLUS + CEUS	0.880	< 0.001	0.799–0.887	0.889	0.750
CDFI + CEUS + AngioPLUS	0.941	< 0.001	0.887–0.996	0.907	0.857

**Table 5.** ROC analysis: invasive lymphoma vs. indolent lymphoma.

**Conclusion**

Obtaining accurate pathological tissue for the early identification of transformed lymphoma before the onset of clinical symptoms is an ongoing endeavour for clinicians. Our study demonstrated that Ultrasonographic Vascular imaging can help identifying invasive and indolent lymphomatous lymph nodes, and CDFI combined with CEUS has the highest diagnostic sensitivity, which can guide clinicians to make more accurate diagnosis.

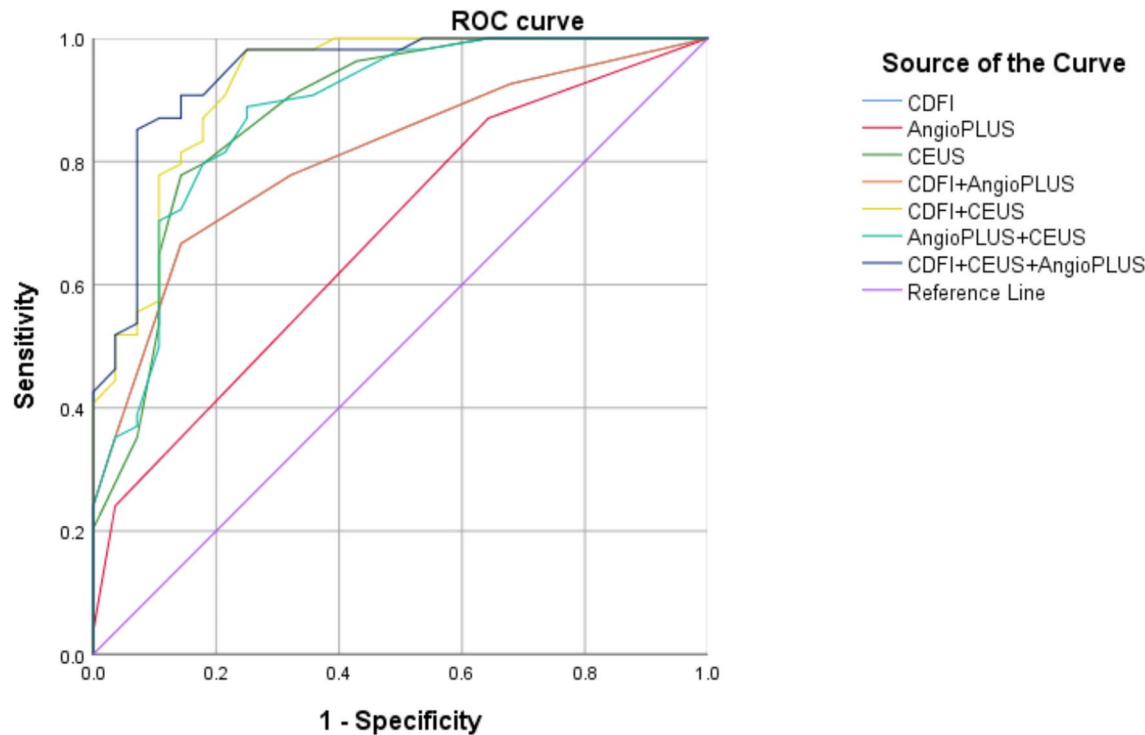


**Fig. 5.** Receiver operating characteristic (ROC) curve for assessing the diagnostic value of different vascular imaging.

	CDFI vs AngioPLUS	CDFI vs CEUS	CDFI + CEUS vs CDFI + AngioPLUS	CDFI + CEUS vs AngioPLUS + CEUS	CDFI + CEUS vs CDFI + CEUS + AngioPLUS	AngioPLUS + CDFI vs CDFI + CEUS + AngioPLUS
Difference between areas	0.132	0.071	0.117	0.044	0.017	0.134
95%CI	0.034 to 0.230	− 0.035 to 0.176	0.040 to 0.193	− 0.006 to 0.09	− 0.013 to 0.046	0.046 to 0.221
P value	0.009	0.189	0.003	0.086	0.261	0.003

**Table 6.** A precise comparison of the diagnostic accuracy of different ultrasound techniques.

Data availability

The datasets used and/or analysed during the current study available from the corresponding author on reasonable request.

Received: 28 May 2024; Accepted: 7 March 2025  
Published online: 22 March 2025

References

1. Alaggio, R. et al. The 5th edition of the World Health Organization classification of haematolymphoid tumours: Lymphoid neoplasms. *Leukemia* **36**(7), 1720–1748. <https://doi.org/10.1038/s41375-022-01620-2> (2022).

2. Mayerhoefer, M. E., Umutlu, L. & Schöder, H. Functional imaging using radiomic features in assessment of lymphoma. *Methods* **188**, 105–111. <https://doi.org/10.1016/j.ymeth.2020.06.020> (2021).

3. Schürch, C. M., Federmann, B., Quintanilla-Martinez, L. & Fend, F. Tumor heterogeneity in lymphomas: A different breed. *Pathobiology* **85**(1–2), 130–145. <https://doi.org/10.1159/000475530> (2018).

4. Godfrey, J., Leukam, M. J. & Smith, S. M. An update in treating transformed lymphoma. *Best Pract. Res. Clin. Haematol.* **31**(3), 251–261. <https://doi.org/10.1016/j.beha.2018.07.008> (2018).

5. McKay, M. J., Taubman, K. L., Lee, S. & Scott, A. M. Radiotherapy planning of lymphomas: Role of metabolic imaging with PET/CT. *Ann. Nucl. Med.* **36**(2), 162–171. <https://doi.org/10.1007/s12149-021-01703-7> (2022).

6. Ma, X. et al. Application of contrast-enhanced ultrasound (CEUS) in lymphomatous lymph nodes: A comparison between PET/CT and CONTRAST-ENHANCED CT. *Contrast Media Mol. Imaging* **2019**, 5709698. <https://doi.org/10.1155/2019/5709698> (2019).

7. Jørgensen, J. M. et al. Angiogenesis in non-Hodgkin's lymphoma: Clinico-pathological correlations and prognostic significance in specific subtypes. *Leuk Lymphoma* **48**(3), 584–595 (2007).

8. Farinha, P. et al. Vascularization predicts overall survival and risk of transformation in follicular lymphoma. *Haematologica* **95**(12), 2157–2160. <https://doi.org/10.3324/haematol.2009.021766> (2010).

9. Chiorean, L. et al. Clinical value of imaging for lymph nodes evaluation with particular emphasis on ultrasonography. *Zeitschrift für Gastroenterologie* **54**(8), 774–790. <https://doi.org/10.1055/s-0042-108656> (2016).
10. Gloger, M. et al. Lymphoma angiogenesis is orchestrated by noncanonical signaling pathways. *Cancer Res.* **80**(6), 1316–1329. <https://doi.org/10.1158/0008-5472.CAN-19-1493> (2020).
11. Menzel, L., Höpken, U. E. & Rehm, A. Angiogenesis in lymph nodes is a critical regulator of immune response and lymphoma growth. *Front. Immunol.* **11**, 591741. <https://doi.org/10.3389/fimmu.2020.591741> (2020).
12. Dangore, S. B., Degwekar, S. S. & Bhowate, R. R. Evaluation of the efficacy of colour Doppler ultrasound in diagnosis of cervical lymphadenopathy. *Dento Maxillo Fac. Radiol.* **37**(4), 205–212. <https://doi.org/10.1259/dmfr/57023901> (2008).
13. Jung, H. K., Park, A. Y., Ko, K. H. & Koh, J. Comparison of the diagnostic performance of power doppler ultrasound and a new microvascular doppler ultrasound technique (AngioPLUS) for differentiating benign and malignant breast masses. *J. Ultrasound Med.* **37**(11), 2689–2698. <https://doi.org/10.1002/jum.14602> (2018).
14. Dudau, C. et al. Can contrast-enhanced ultrasound distinguish malignant from reactive lymph nodes in patients with head and neck cancers?. *Ultrasound Med. Biol.* **40**(4), 747–754. <https://doi.org/10.1016/j.ultrasmedbio.2013.10.015> (2014).
15. Xin, L. et al. Parameters for contrast-enhanced ultrasound (CEUS) of enlarged superficial lymph nodes for the evaluation of therapeutic response in lymphoma: A preliminary study. *Med. Sci. Monit. Int. Med. J. Exp. Clin. Res.* **23**, 5430–5438 (2017).
16. Ahuja, A. & Ying, M. An overview of neck node sonography. *Invest. Radiol.* **37**(6), 333–342 (2002).
17. Adler, D. D., Carson, P. L., Rubin, J. M. & Quinn-Reid, D. Doppler ultrasound color flow imaging in the study of breast cancer: Preliminary findings. *Ultrasound Med. Biol.* **16**(6), 553–559 (1990).
18. Son, M. J. et al. Can ultrasonographic vascular and elastographic features of invasive ductal breast carcinoma predict histologic aggressiveness?. *Acad. Radiol.* **27**(4), 487–496. <https://doi.org/10.1016/j.acra.2019.06.009> (2020).
19. Jiang, W. et al. Value of contrast-enhanced ultrasound and PET/CT in assessment of extramedullary lymphoma. *Eur. J. Radiol.* **99**, 88–93. <https://doi.org/10.1016/j.ejrad.2017.12.001> (2018).
20. Niu, X. et al. Comparison of contrast-enhanced ultrasound and positron emission tomography/computed tomography (PET/CT) in lymphoma. *Med. Sci. Monit.* **24**, 5558–5565. <https://doi.org/10.12659/MSM.908849> (2018).
21. Chhabra, A. et al. Conventional MR and diffusion-weighted imaging of musculoskeletal soft tissue malignancy: Correlation with histologic grading. *Eur. Radiol.* **29**(8), 4485–4494. <https://doi.org/10.1007/s00330-018-5845-9> (2019).
22. Perry, A. M. et al. A new biologic prognostic model based on immunohistochemistry predicts survival in patients with diffuse large B-cell lymphoma. *Blood* **120**(11), 2290–2296. <https://doi.org/10.1182/blood-2012-05-430389> (2012).
23. Kataria, S. P., Malik, S., Yadav, R., Kapil, R. & Sen, R. Histomorphological and morphometric evaluation of microvessel density in nodal non-hodgkin lymphoma using CD34 and CD105. *J. Lab. Phys.* **13**(1), 22–28. <https://doi.org/10.1055/s-0041-1726569> (2021).
24. Sabaté-Llobera, A. et al. Low-dose PET/CT and full-dose contrast-enhanced CT at the initial staging of localized diffuse large B-cell lymphomas, clinical medicine insights. *Blood Disord.* **9**, 29–32. <https://doi.org/10.4137/CMBD.S38468> (2016).
25. Gómez León, N. et al. Multicenter comparison of contrast-enhanced FDG PET/CT and 64-slice multi-detector-row CT for initial staging and response evaluation at the end of treatment in patients with lymphoma. *Clin. Nucl. Med.* **42**(8), 595–602. <https://doi.org/10.1097/RLU.0000000000001718> (2017).
26. Giovagnorio, F., Galluzzo, M., Andreoli, C., De, C. M. L. & David, V. Color Doppler sonography in the evaluation of superficial lymphomatous lymph nodes. *J. Ultrasound Med.* **21**(4), 403–408 (2002).
27. Esen, G. Ultrasound of superficial lymph nodes. *Eur. J. Radiol.* **58**(3), 345–359 (2006).
28. Ying, M., Ahuja, A. & Brook, F. Accuracy of sonographic vascular features in differentiating different causes of cervical lymphadenopathy. *Ultrasound Med. Biol.* **30**(4), 441–447 (2004).
29. Ahuja, A. & Ying, M. Sonography of neck lymph nodes. Part II: abnormal lymph nodes. *Clin. Radiol.* **58**(5), 359–366 (2003).
30. Nie, J. et al. The value of CEUS in distinguishing cancerous lymph nodes from the primary lymphoma of the head and neck. *Front. Oncol.* **10**, 473. <https://doi.org/10.3389/fonc.2020.00473> (2020).
31. Ribatti, D., Nico, B., Ranieri, G., Specchia, G. & Vacca, A. The role of angiogenesis in human non-Hodgkin lymphomas. *Neoplasia (New York, N.Y.)* **15**(3), 231–238 (2013).
32. Yoo, J., Je, B. K. & Choo, J. Y. Ultrasonographic demonstration of the tissue microvasculature in children: Microvascular ultrasonography versus conventional color doppler ultrasonography. *Korean J. Radiol.* **21**(2), 146–158. <https://doi.org/10.3348/kjr.2019.0500> (2020).
33. Kratzer, W. et al. Comparison of superb microvascular imaging (SMI) quantified with ImageJ to quantified contrast-enhanced ultrasound (qCEUS) in liver metastases—a pilot study. *Quant. Imaging Med. Surg.* **12**(3), 1762–1774. <https://doi.org/10.21037/qims-21-383> (2022).
34. Moghimirad, E., Bamber, J. & Harris, E. Plane wave versus focused transmissions for contrast enhanced ultrasound imaging: the role of parameter settings and the effects of flow rate on contrast measurements. *Phys. Med. Biol.* **64**(9), 095003. <https://doi.org/10.1088/1361-6560/ab13f2> (2019).
35. Fetzer, D. T. et al. Artifacts in contrast-enhanced ultrasound: A pictorial essay. *Abdom. Radiol. (NY)* **43**(4), 977–997. <https://doi.org/10.1007/s00261-017-1417-8> (2018).

## Acknowledgements

We thank all the patients who participated in this study.

## Author contributions

Lin Li and Wenjuan Lu have contributed equally to this work and share first authorship. \*Corresponding author: Pingyang Zhang\* and Xinhua Ye\*. Wenjuan Lu: Data curation, Formal analysis, Investigation, Methodology, Writing – original draft. Lin Li: Data curation, Formal analysis, Investigation, Methodology, Writing – original draft. Hongyan Deng: Data curation, Formal analysis, Investigation. Wenqin Chen: Data curation, Formal analysis, Investigation. Hua Shu: Resources, Validation, Investigation. Pingyang Zhang: Conceptualization, Methodology, Project administration, Resources, Supervision, Validation, Writing – review & editing. Xinhua Ye: Conceptualization, Methodology, Project administration, Resources, Supervision, Validation, Writing – review & editing.

## Declarations

## Competing interests

The authors declare no competing interests.

## Ethical statement

The authors are accountable for all aspects of the work in ensuring that questions related to the accuracy or

integrity of any part of the work are appropriately investigated and resolved. The study protocol adheres to the 1964 Helsinki Declaration and its successive emendations and was approved by the local ethics committee (approval ID: 2022-SR-058). Written informed consent was obtained from the patient for publication of this study and any accompanying images.

### Additional information

**Correspondence** and requests for materials should be addressed to P.Z. or X.Y.

**Reprints and permissions information** is available at [www.nature.com/reprints](http://www.nature.com/reprints).

**Publisher's note** Springer Nature remains neutral with regard to jurisdictional claims in published maps and institutional affiliations.

**Open Access** This article is licensed under a Creative Commons Attribution-NonCommercial-NoDerivatives 4.0 International License, which permits any non-commercial use, sharing, distribution and reproduction in any medium or format, as long as you give appropriate credit to the original author(s) and the source, provide a link to the Creative Commons licence, and indicate if you modified the licensed material. You do not have permission under this licence to share adapted material derived from this article or parts of it. The images or other third party material in this article are included in the article's Creative Commons licence, unless indicated otherwise in a credit line to the material. If material is not included in the article's Creative Commons licence and your intended use is not permitted by statutory regulation or exceeds the permitted use, you will need to obtain permission directly from the copyright holder. To view a copy of this licence, visit <http://creativecommons.org/licenses/by-nc-nd/4.0/>.

© The Author(s) 2025